Georgia Tech Space Systems Design Laboratory

Development of a Cubesat-Scale Green Monopropellant Propulsion System for NASA's Lunar Flashlight Mission

AE 8900 Special Problems Report

Author: Grayson Huggins
Advisor: Dr. E. Glenn Lightsey

Space Systems Design Laboratory
Daniel Guggenheim School of Aerospace Engineering
Georgia Institute of Technology

July 29, 2020

Development of a CubeSat-Scale Green Monopropellant Propulsion System for NASA's Lunar Flashlight Mission

Grayson Huggins* and E. Glenn Lightsey†
Georgia Institute of Technology, Atlanta, Georgia, 30313

NASA's Lunar Flashlight is a low-cost 6U CubeSat whose mission is to search for ice and mineral deposits inside of the scattered craters at Moon's southern pole. To conduct its primary science mission, Lunar Flashlight must be placed in a stable lunar polar orbit which requires utilization of an on-board propulsion system. However, to this date most CubeSats have been propelled by cold-gas or electric propulsion systems that have proven to scale well, but are not efficient or impulsive enough to conduct large ΔV maneuvers such as orbit insertions. To this end, the Lunar Flashlight mission has chosen to utilize a custom-designed green monopropellant propulsion system developed by the Georgia Institute of Technology under the sponsorship and guidance of NASA's Marshall Spaceflight Center and Jet Propulsion Laboratory. The developed system is capable of providing more than the required propulsive capability for full mission success while fitting inside of a 2.5U volume and weighing less than six kilograms. The system is developed for use with the AF-M315E green monopropellant that provides higher specific impulse compared to traditional hydrazine while also being safer to handle. If successful, the presented propulsion system will enable Lunar Flashlight to be the first CubeSat to reach the Moon, the first to conduct an orbit insertion, and will be the second-ever spaceflight demonstration of the AF-M315E propellant.

I. SSDL Spacecraft Propulsion Background

Before describing the propulsion system development effort, it is important to distinguish between the two types of propulsion systems that have been developed by the Glenn Lightsey Research Group in the Georgia Tech Space Systems Design Lab. Understanding these systems will help to explain why the Lunar Flashlight mission decided to develop a green-monopropellant system, as well as understand some of the challenges faced when attempting to scale this system down to the size of a 6U CubeSat.

A. Cold-Gas

Cold-gas propulsion systems function solely on pressure-driven gas flow through a nozzle to generate thrust, with no chemical reactions to release the energy stored in the chemical bonds of the propellant. There are five main components: a tank, plenum, valves, nozzle, and the structure itself. Similar to other propulsion systems, the propellant tank is designed to maximize the system's total capability by holding the maximum amount of propellant. The propellant is stored in its liquid state as a liquid is much more dense than a gas. However, for thrust to be generated the nozzles need the propellant flowing to them in a gaseous state, as gases take the shape of the geometry around them which allows a flowing gas to be compressed and expanded in a converging-diverging nozzle. Additionally, the gas pressure pushes the flow through the system, so refrigerants are typically used as cold-gas propellants because of their high liquid density and high vapor pressure. Therefore, the propellant is split between liquid and gaseous states, with the gas being present at its vapor pressure as a function of temperature. The control logic of these systems is described well by Wilk and Lightsey [1].

Cold-gas systems are quite simple mechanically and electronically when compared with other systems like liquid bi-propellant. This allows them to be developed quickly and have very low mass, which is a big plus for rapid development, low mass and low cost missions such as CubeSats. Additionally, the onset of 3D printing technology for use in space applications has allowed engineers to design cold-gas systems down to smaller scales, to the point that there are 0.5U cold-gas systems that have been flown. The drawback is that cold-gas systems are very inefficient at 40-60 I_{sp}, and the smaller they get the less capability they have. Therefore, to this date most cold-gas systems are

*Graduate Research Assistant, Daniel Guggenheim School of Aerospace Engineering, ghuggins3@gatech.edu
†Professor, Daniel Guggenheim School of Aerospace Engineering, glenn.lightsey@gatech.edu

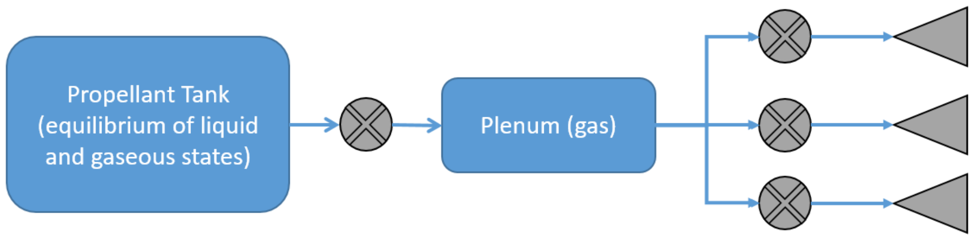

Fig. 1 Cold-gas propulsion system fluid schematic

mainly used for small delta-V or attitude-control maneuvers, and are incapable of providing the necessary impulse for large maneuvers. However, most Earth-orbiting CubeSats missions do not require large orbit maneuvers and find their propulsion needs can be covered well by cold-gas systems. Some examples of cold-gas propulsion systems built by GLRG and their capabilities are shown in Table 1.

Mission	Mass	Total Impulse
PROX-1	6.000 kg	998.9 N-s
BioSentinel	1.265 kg	36 N-s
ASCENT	3.660 kg	549.1 N-s
Bevo-2	0.380 kg	48.9 N-s

Table 1 Heritage cold-gas systems [2]

B. Liquid Monopropellant

Different than cold-gas, liquid monopropellant systems take advantage of the chemical energy stored inside of a propellant's molecules to add energy to the flow before being accelerated through a nozzle. Many industrial and aerospace systems that require chemical energy release rely on the process of combustion, where a fuel and oxidizer are joined at the right conditions and react exothermically, adding energy to the system. However, as the name suggests monopropellants only have one propellant, so combustion is not utilized. Instead, the chemical energy stored in the monopropellant is released using catalytic decomposition. When the monopropellant is exposed to a catalyst bed at a specified temperature, the catalyst breaks down the liquid monopropellant molecules in an exothermic reaction that adds energy to the system as well as converting the liquid to a gas. As a direct analog to cold gas propulsion systems, adding this energy to the propellant flow allows monopropellant systems to use less propellant to generate the same amount of thrust as a cold-gas system, increasing its efficiency as quantified by I_{sp}. Therefore, a monopropellant system that has the same capability as a cold-gas system would have a smaller propellant tank. Because of this feature, monopropellant systems have been and continue to be widely used on many different spacecraft and launch vehicles.

However, the types of monopropellants are vastly different than cold-gas propellants. Monopropellants are engineered to have the best performance traits (high energy density, easy to manufacture, etc.) and are very uncommon for use in daily activities, unlike the refrigerants used for many cold-gas systems. Therefore, these propellants are typically not engineered for high levels of safety and are usually very hazardous and difficult to handle. As an extreme example, in Figure 2 a technician is fueling the MESSENGER spacecraft with the commonly-used monopropellant hydrazine, who has to wear a full suit to handle the propellant during loading. Due to the extremely hazardous nature of hydrazine, the past few decades have seen a push in development of safer monopropellants with similar performance, if not better, compared to hydrazine. These "green" monopropellants are typically based off of hydroxyl-ammonium nitrate (HAN), ammonium dinitramide (ADN), or hydrogen peroxide. Although these propellants are considered safer to handle than hydrazine, they are still quite dangerous to humans and have to be handled with care.

Traditionally, monopropellant systems have been designed via pressure-fed (blowdown) or pump-fed fluid schematics. A simplified version of a blowdown schematic is seen in Figure 3, showing propellant fluid tubing, propellant management device (PMD) location and the heated catalytic decomposition chamber of the thruster, shown by $\dot{q}$. Blowdown

Fig. 2 A technician loads hydrazine onto the MESSENGER spacecraft, Credit: NASA/Johns Hopkins APL

schematics are widely used on larger-scale propulsion systems as they are relatively simple in electrical and control design, but present unique problems when scaled down to the size of a CubeSat. Blowdown systems require structurally strong propellant tanks capable of withstanding high pressure loading throughout the mission lifetime without introducing plastic deformation or failure. Typically, cylindrical or spherical tanks are used for these and other high-pressure systems to evenly distribute pressure loading around the structure, and the wall thickness is scaled to match anticipated loading along with required factors of safety. CubeSats, as described by their name, are inherently rectangular in shape and are standardized around the industry in terms of unit volume, or 1U, which is a 10 cm x 10 cm x 10 cm cube. Therefore, the propulsion system is required to fit in a rectangular envelope and cannot efficiently mold its tank into a round shape for improved strength. The sharp corners in a rectangular prism hinder the structure's ability to distribute pressure loading, causing high stress concentrations. Distributing the stress requires additional wall thickness or increasingly complicated structural design. For this reason, designing a pressure vessel in a CubeSat form factor capable of withstanding the necessary pressures of a blowdown system would require a complex and/or massive structure. This design would limit the amount of propellant that could be loaded while also meeting the very low mass and volume requirements typical of CubeSat missions, overall limiting the propulsive capability of the system.

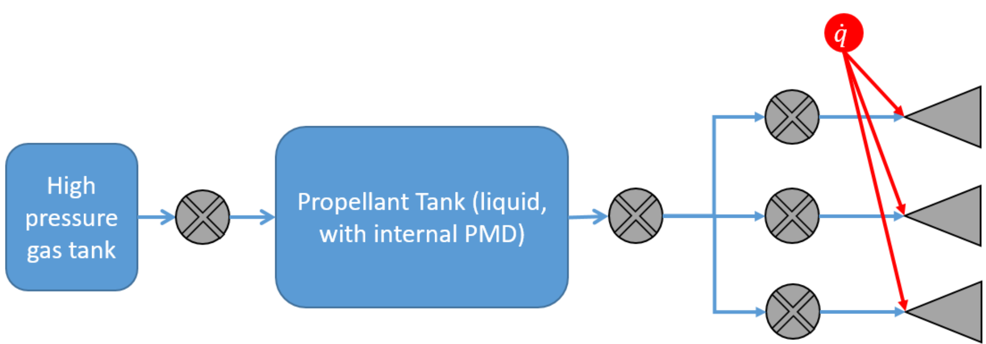

Fig. 3 Blowdown monopropellant propulsion system fluid schematic

The pump-fed schematic offers a promising alternative to the blowdown schematic for use on CubeSat applications, shown in Figure 4. A pump is added to the system which is placed between the propellant tank and thruster to pull propellant from the tank and deliver it to the monopropellant thrusters. The addition of a pump reduces the necessary system pressures to more manageable levels and decreases the complexity of the propellant tank structural design and overall system mass. However, significant complexity is added to the tubing, controller electronics and software. The pump speed-up process prior to firing requires that the propellant be able to recirculate, adding new routing and a flow control device (FCD). Additionally, the electronic control system must now consider system sensor readings to vary the pump's rotational speed throughout the thruster conditioning and firing phases to ensure proper flow rate and system pressures. An example of where a pressure sensor could be placed in the fluid routing for this control logic to function is shown in green below.

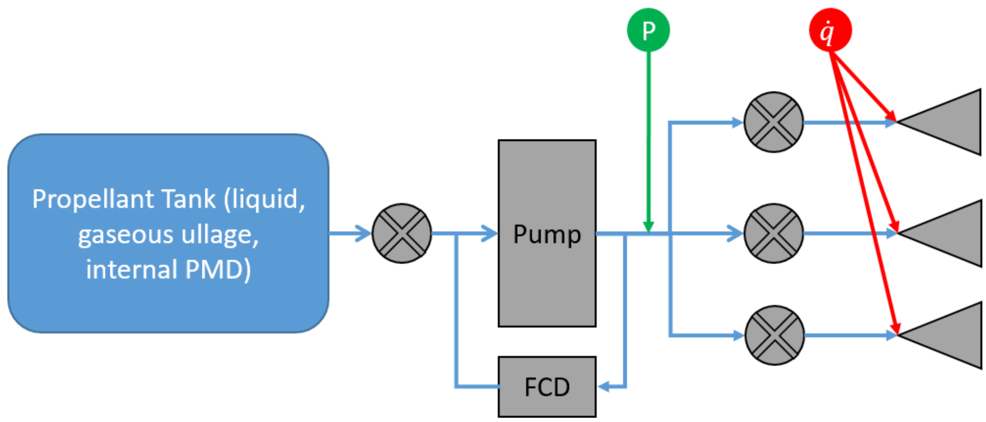

Fig. 4 Pump-fed monopropellant propulsion system fluid schematic

II. Lunar Flashlight Mission

Lunar Flashlight is an upcoming 6U CubeSat mission from NASA's Jet Propulsion Laboratory that will search for water-ice deposits and other volatiles near the lunar south pole from a highly-eccentric polar lunar orbit [3]. Lunar Flashlight will fly on the Artemis I mission as part of a group of small satellites that will be deployed by the Space Launch System (SLS) on its journey around the Moon. Except for the JPL MarCO CubeSats that flew by Mars in November 2018, CubeSats have been mostly limited to Earth orbiting missions until now. Lunar Flashlight aims to add to the flight experience of deep-space CubeSats and demonstrate their ability to conduct space science missions at a fraction of the cost and complexity of larger missions. Lunar Flashlight will conduct an orbit insertion at the Moon using a green monopropellant propulsion system developed uniquely for this mission, fueled by the AF-M315E propellant developed by the Air Force Research Laboratories (AFRL). The custom designed propulsion system developed by a team from NASA's Marshall Spaceflight Center (MSFC) and Georgia Tech's Space Systems Design Laboratory (SSDL) delivers over 2500 N-s of total impulse for the orbit insertion and necessary attitude maneuvers, fits within a 2.5U volume, and has a total wet mass under six kilograms. Upon completion, Lunar Flashlight may become the first CubeSat to achieve orbit around a planetary body besides the Earth, which is enabled by the new propulsion system.

The LFPS consists of a propellant tank, propellant management device (PMD), manifold, pump, four AF-M315E thrusters, and several micro-fluidic components developed by NASA MSFC. Additive manufacturing is utilized to fabricate the PMD and manifold to the scale that is necessary within a CubeSat form factor. The PMD and manifold designs require a complex geometry that would be impossible to machine using traditional methods. Additionally, the manifold incorporates all necessary fluid paths and mechanical interfaces into a single continuous structure, which significantly decreases the total volume and mass of the system. The LFPS unit notional location in the Lunar Flashlight spacecraft is shown in in Figure 6.

A. ConOps

Lunar Flashlight is stowed during launch in a 6U CubeSat deployer in the second stage of the SLS rocket, underneath the Orion capsule. After lunar transfer orbit-insertion and Orion deployment, Lunar Flashlight's deployer will release the spacecraft on its journey to the Moon. The propulsion system will be turned on for the first time immediately following release, and conduct a small maneuver as a system-checkout. The spacecraft will proceed to perform three fly-bys of the

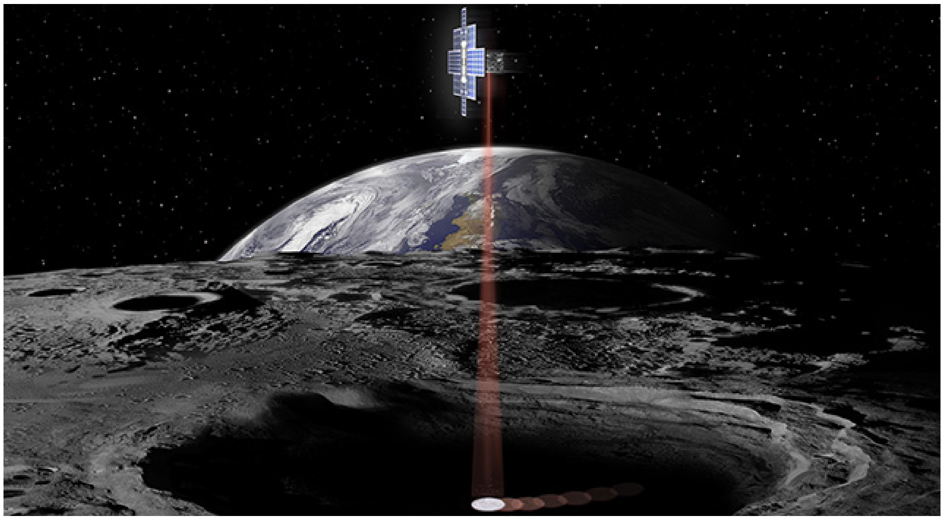

Fig. 5 Artist concept of Lunar Flashlight conducting its primary science mission at the Lunar south pole. Image credit: NASA/JPL-Caltech

Moon over the next 90 days, occasionally performing impulsive maneuvers along the way. On the fourth trip to the Moon, the propulsion system will complete its largest manuever to enter into polar Lunar orbit, with a perilune at the south pole of 15 kilometers and an orbital period around 7 days. Over the next two months, 10 science passes around the south pole will be conducted, where the spacecraft will utilize its instruments to collect and send data back to Earth. During this time the propulsion system will mainly be used for attitude maneuvers and momentum wheel desaturation. After the science goals of the mission have been concluded, including possible mission extension(s), the propulsion system will perform a final burn to place the spacecraft on an impact trajectory with the lunar surface for disposal.

B. Technology Demonstration

With CubeSat technology becoming more feasible for deep-space applications comes the need for more efficient and impulsive small-scale propulsion systems. As stated before, most CubeSats have been limited to low-earth orbit but additional propulsive capability would allow this class of spacecraft to visit further destinations and extend mission lifetimes.

The mission also serves as a first flight of a multitude of custom micro-valves developed by NASA MSFC, with the intention that they will be used on many other NASA CubeSat propulsion systems after a successful demonstration on the LFPS. Additionally considered is the use of COTS components in the design, which shows how these small-satellite systems can be built without designing the whole system from sractch. The pump used is modified from a commercial micro-pump developed by Flight Works Inc. (2212-M04X09) and the electronics boards are built from COTS components.

Lunar Flashlight is a testament to how small satellites can act as testbeds for many new technologies in a rapid, cost-effective way while also expanding our understanding of our solar system and beyond. However, with new innovation come new challenges, so the following sections will focus on discussing the challenges that were faced in the various phases of the project to build the system to its scale and meet its goals.

III. Propulsion System

A. Propulsion Schematic and Requirements

Before beginning design of the propulsion system, the LFPS project had to choose between a blowdown or pump-fed system by considering each schematic's trade between total mass, volume, performance, and overall system complexity, as discussed in Section I.B. Additionally considered in this discussion and trade were safety and fracture control. The high pressures of a blowdown system coupled with the hazardous nature of the propellant would require significant structural analysis and testing to clear the necessary control review boards [4]. A pump-fed system reduces the system

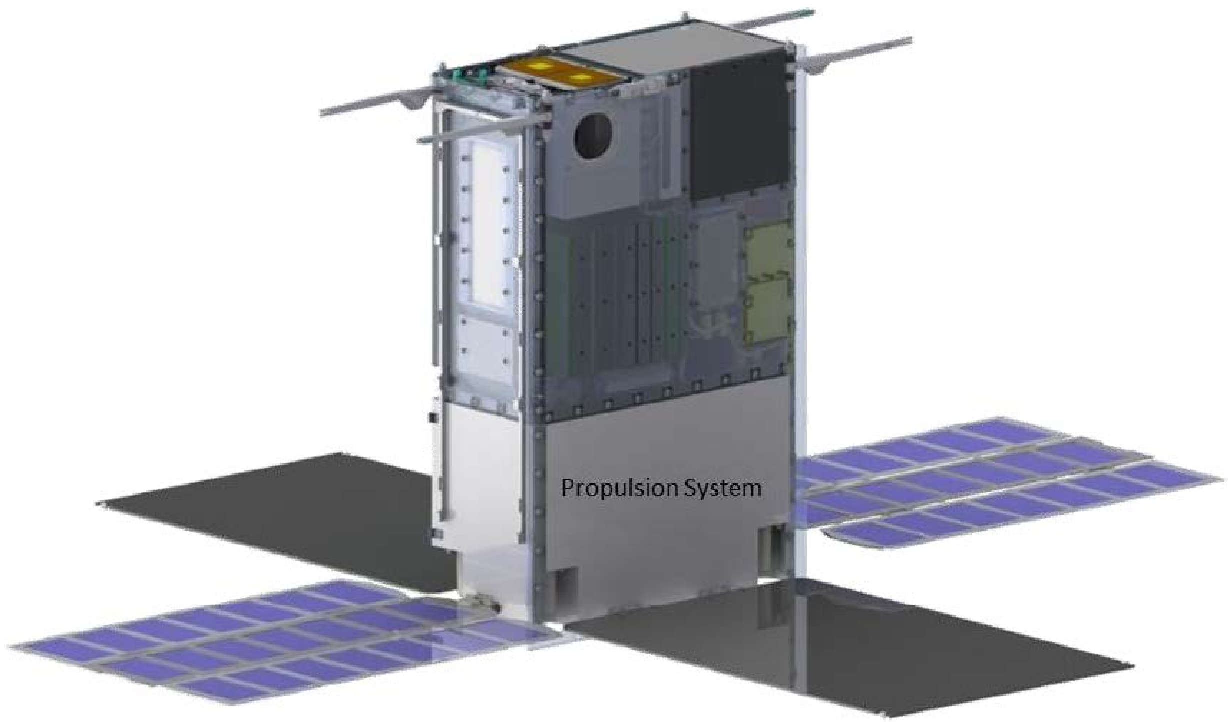

Fig. 6 Lunar Flashlight spacecraft, specifying the location of the propulsion system

pressures to below the launch vehicle's pressure vessel classification (100 psia), which significantly reduces the concern of safety control and fracture criticality. For these reasons, the LFPS team selected a pump-fed propulsion schematic, as shown in Figure 7. However, the project still conducted significant reviews to reclassify the propellant tank's risk from a catastrophic to critical failure. This reduced risk classification allowed the design to remove a redundant isolation valve, and limited two-fault tolerant fluid seals to be necessary only to the propellant tank. Meanwhile, all component seals to the manifold could be designed to single-fault tolerance [4]. This classification was reviewed and approved due to the AF-M315E propellant's high viscosity and practically non-existent vapor pressure that would prevent high leakage and self-pressurization, which could lead to safety or fracture hazards before and during launch [5].

In the selected pump-fed configuration, the propellant tank is filled with AF-M315E, a gaseous nitrogen ullage for pressurization, the propellant management device (PMD), a fill/drain valve, pressure transducer, and various heaters and thermocouples. The propellant tank is isolated from the rest of the system by the propellant isolation valve, which is one of the new micro-solenoid valves developed by NASA MSFC for CubeSat propulsion systems. When the isolation valve is opened, the combination of the ullage and operating pump pull propellant from the tank and increase the fluid pressure from storage pressure (70 psia) to the thruster operating pressure (350 psia). During firing, the propellant flows through the opened micro-solenoid thruster valves and into the thrusters for firing and thrust. Prior to firing, the thruster valves are closed and the fluid instead flows through a recirculation loop that carries the propellant exiting the pump through a fixed orifice flow control device (FCD) and back to the pump inlet.

Georgia Tech's SSDL was contracted to design the LFPS structure to conform to the required interfaces and envelopes described by the Lunar Flashlight project at JPL. Table 2 lays out a few of the propulsion system requirements provided to Georgia Tech by MSFC and JPL. Figure 8 shows the LFPS flight configuration that meets all the requirements, and whose components are being manufactured simultaneously with this submission.

B. Control

During nominal operation after the initial firing, the manifold fluid lines contain propellant between burns. The propulsion system begins its operation by commanding the thruster catalyst bed to heat up to operating temperatures via thermostatic control, called thruster conditioning, which could last for 10-30 minutes depending on the current thermal

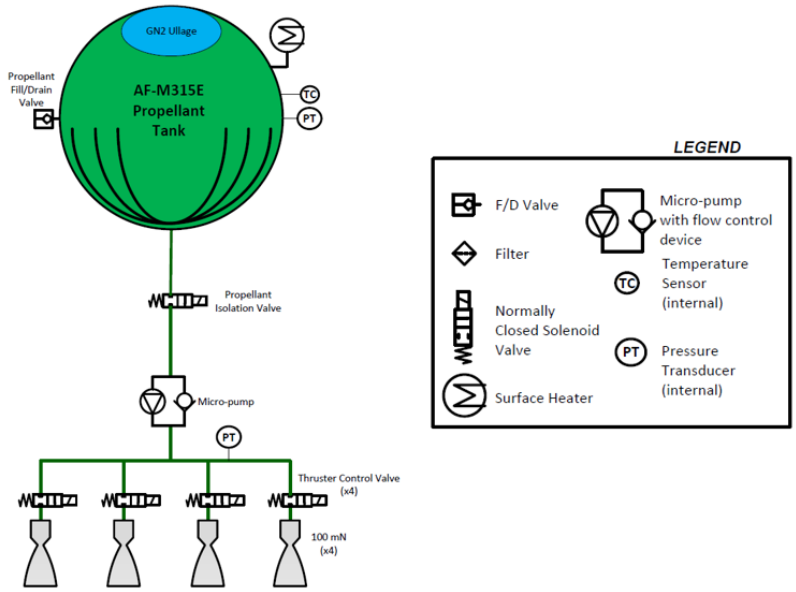

Fig. 7 Lunar Flashlight Propulsion System, fluid and mechanism propulsion schematic

Table 2 LFPS Level 4 System Requirements (LFPS-SPEC-204)

Requirement	Description	Notes
LFPS-REQ-005	Wet Mass	The propulsion system's ‘wet’ mass shall not exceed 5.55kg
LFPS-REQ-006	Total Impulse	The total impulse capability for the system shall be no less than 1800 Ns
LFPS-REQ-011	Propellant Tank MDP	The propellant tank shall be designed for a Maximum Design Pressure (MDP) of 100 psia
LFPS-REQ-012	Manifold MDP	The manifold shall be designed for a Maximum Design Pressure (MDP) of 500 psia
LFPS-REQ-013	Design Factor	The propulsion system shall have all pressurized hardware designed, analyzed, and tested to the following pressures in accordance with NASA-STD-5001. Proof pressure = 1.5 times MDP, Burst Pressure = 2.5 times MDP
LFPS-REQ-025	System External Leakage Rate Allowable	The external leakage rate of the system shall be no greater than $5e^{-3}$ SCCS GHe at MDP

environment. In the last minute of thruster conditioning, the pump accelerates to operating rotational velocity. During this transient, the thruster valves remain closed to prevent any propellant flowing to the thrusters, which would either be below operating pressure or below catalyst operating temperature. The thruster valves are only opened when the entire system is ready to fire, which the system performs via control from the spacecraft attitude-control system (ACS). Therefore, during pump acceleration the propellant inside of the manifold has nowhere to easily go. This issue is solved by creating a recirculation loop between the pump's outlet and inlet, where the fluid instead flows through a fixed orifice flow control device. The orifice adds resistance to the flow by restricting it to a small area, and when pressures or flow rates are high enough the fluid overcomes this resistance and flows through the orifice that routes back to the pump inlet. Figure 9 shows the recirculation loop and it's routing inside of the system.

During nominal firing, the propellant isolation valve and thruster valve(s) are opened. The outlet flow rates of

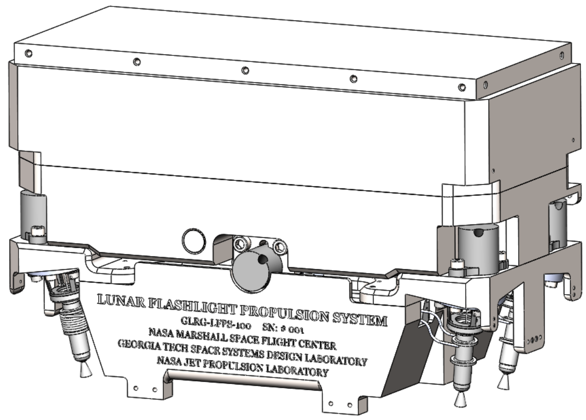

Fig. 8 Isometric view of the Lunar Flashlight Propulsion System model

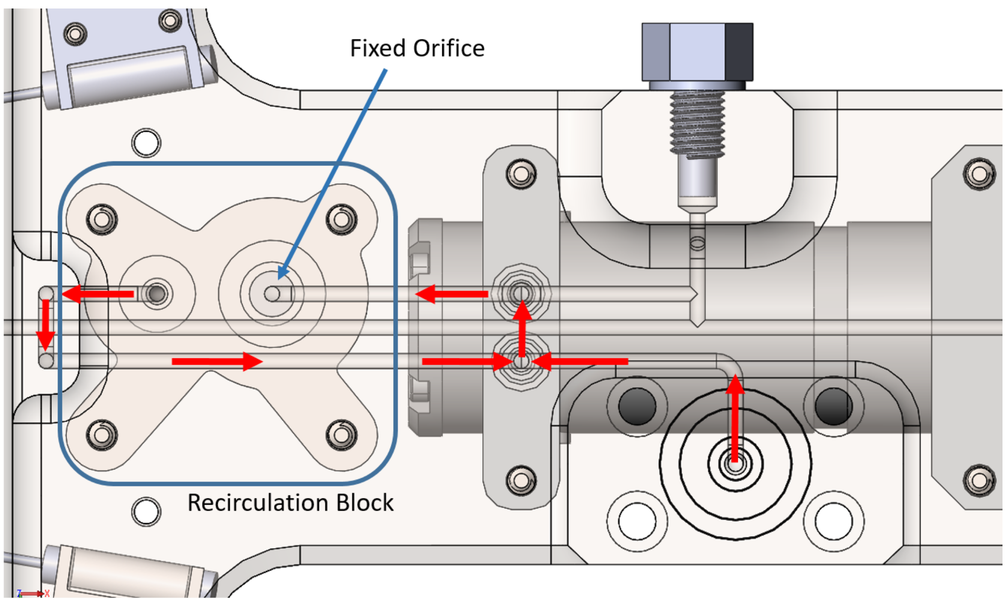

Fig. 9 Recirculation loop

the COTS pump are larger than what the four thrusters can handle, so a majority of the propellant flows through the recirculation loop during firing. However, a small portion of the propellant is now able to flow through passages to each thruster valve. The open thruster valve exposes the propellant to space and pressure differential pushes the propellant through the heated thruster catalytic decomposition chamber and expels it, providing a nominal 100 mN thrust per thruster. During the mission lifetime, any number of the four thrusters are available to be operated simultaneously based on the desired maneuver, as controlled by the valve drive electronics.

IV. Mechanical Design

A. Propellant Tank

All major structures of the propulsion system, including the propellant tank, are made from Grade 5 Titanium (Ti-6Al-4V) which has high strength-to-weight ratio (SWR) and is resistant to corrosion, which is necessary for long-term exposure with the AF-M315E propellant. This titanium alloy has been used extensively on heritage monopropellant systems, such as the GPIM propellant tank [6].

An early idea considered for the tank design was to additively manufacture (AM) the propellant tank and manifold into one single continuous structure of printed Ti-6Al-4V. The as-printed structure would contain the propellant storage volume, necessary fluid passages and the propellant management device. Precision interfaces or thread-forms would be machined into the as-printed structure, typical of many metal printed parts. However, the striated nature of an additively manufactured part's macro-structure led to the concern of micro-fractures being introduced into the the pressurized tank's material from project stages ranging from manufacturing to flight [2]. These micro-fractures could possibly lead to part failure during flight and this was deemed to be an unacceptable risk. Therefore, the LFPS propellant tank utilizes traditional manufacturing techniques. However, with upcoming technological advances and the expected increased flight heritage of AM, future CubeSat-scale propulsion systems could utilize more system-comprehensive additively manufactured structures that would greatly decrease the number of components and fluid seals throughout the system.

The flight LFPS tank design consists of two traditionally manufactured parts that are electron-beam welded around a weld-line, shown in Figure 10 below prior to welding. The tank top structure contains a majority of the Lunar Flashlight spacecraft interfaces along its outer edge, while internally featuring structural ribbing which prevents unacceptable deformation at MDP that could harm interfacing spacecraft components. In addition to structural support, the ribs solve the issue of fastener feature depth that was encountered many times during the system's mechanical design. Adequate thread engagement is important for ensuring mechanical connection while not stressing the fastener to plastic deformation or failure during torquing, vibration, or other loading. However, the small scale of the system often limited manufacturing tap and thread depth, in this case to keep a minimum wall thickness of three millimeters around the entire tank structure. By placing these ribs directly above the spacecraft interfaces, the interface fastener holes could be drilled and tapped further to allow proper thread engagement while maintaining wall thickness requirements. This issue was encountered often during the LFPS design phase and required the introduction of new features to increase thread engagement.

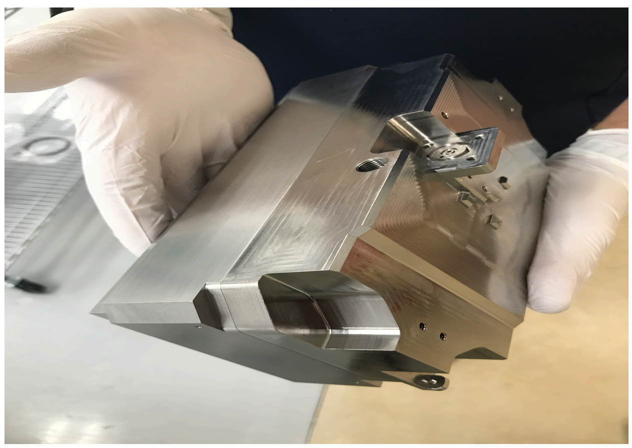

Fig. 10 Flight Propellant Tank Assembly SN 001

The tank bottom structure is a complicated part for its size, containing interface features for nine separate subsystem and spacecraft parts alike while also being designed for total volume and mass requirements. Externally, the tank bottom structure interfaces to the spacecraft and manifold, containing fastening features and small fluid tubing for propellant transfer during operation. The propellant isolation-valve, fill/drain valve, and tank pressure transducer all connect to the exterior in custom designed interfaces. Internally, the structure houses the passive propellant management device (PMD) that forces propellant to the tank's fluid exit tube. Propellant management devices (PMDs) address the issue of zero-gravity fluid management, the physics of which have been extensively studied and implemented on many spaceflight missions [7]. For proper fluid communication, the parts are offset from the surface of the tank bottom structure as suggested by analysis conducted by NASA's Glenn Research Center (GRC). This consideration led to the design of ten fastening bosses symmetrically placed around the internal tank bottom structure. Finally, all internal convex edges are rounded to promote the PMD's operation by preventing surface tension causing the viscous propellant to mass around sharp corners, preventing flow to the tank's fluid exit. The PMD's fit into the tank bottom is shown in Figure 11 below.

The LFPS PMD is made of two parts, the sponge and the vane. The sponge forces propellant towards the fluid exit tube by the principle of liquid surface tension. Prior to exiting from the tank, the propellant must be filtered to prevent any possible foreign-object-debris (FOD) from entering the system's small fluid passages that could damage

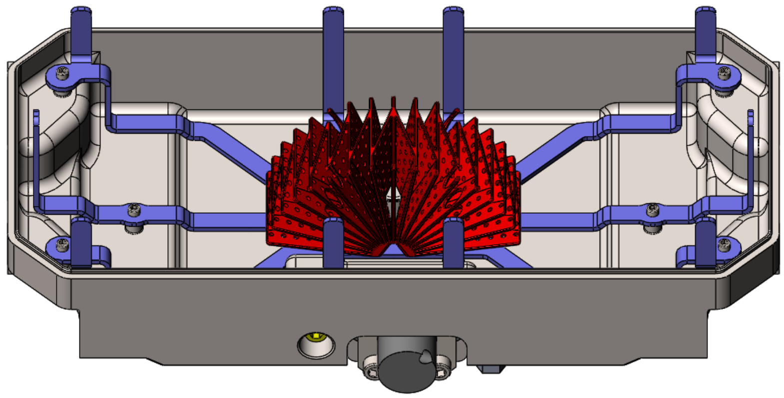

Fig. 11 Tank Bottom Subassembly, showing PMD sponge (red) and vanes (blue)

system components or clog the lines. A COTS ten micron grade 2 titanium filter is placed directly above the fluid exit passage inside of a cutout in the PMD sponge, and preload is applied to the filter using a stack of stainless steel curved disc springs that match the gap between the filter top face and the PMD sponge cutout face. The sponge only covers a portion of the tank's internals, so the PMD vanes are used to bring propellant from outer edges of the tank to the PMD sponge to saturate it.

The complex PMD sponge geometry makes traditional machining extremely challenging. As the sponge is not subject to similar differential pressure loading that presented issues with printing the tank structure, the LFPS project chose to use laser-powder bed fusion (L-PBF) additive manufacturing of Ti-6Al-4V for the PMD sponge structure. Meanwhile, the vanes are not nearly as complex, so they are instead made from Ti-6Al-4V bent sheet metal, and interface between the fastening bosses and PMD sponge.

B. Manifold

The pump-fed propulsion schematic in Figure 7 requires that the fluid be delivered to the pump, thrusters, and a recirculation loop when necessary after exit from the propellant tank. Fluid tubing on traditionally-sized propulsion systems typically use bent metal tubes of varying internal diameters to connect fluid components around the system, but a similar design would be difficult to implement on the LFPS while respecting system mass and envelope requirements.

Additive manufacturing presents a different way of approaching fluid tubing design when compared to these traditional methods. A main advantage of AM is the flexibility of design without having to consider many aspects of design for traditional manufacturing. This is due to the nature of AM versus TM techniques, as the parts are built layer-by-layer rather than by being cut away from a metal stock. Therefore, AM has the ability to print complex, curving passages directly into a structure in a way that is impossible in traditional manufacturing. The GT SSDL has built many cold-gas propulsion systems which print fluid tubing directly into 3D-printed plastic structures, as seen for example on NASA's BioSentinel mission's cold-gas propulsion system [8]. As a technology-demonstration mission coupled with the SSDL's experience with AM on small-scale propulsion systems, the LFPS project chose to manufacture the manifold from L-PBF grade 5 titanium to greatly decrease the system complexity and improve the flight heritage of additively manufactured parts, while presenting relatively low risk to the mission.

Along with the manifold's fluid operation, the manifold also acts as the major interfacing structure of the propulsion system. Figure 12 shows the distribution of system components fastened directly to the manifold. These components rely on traditional fastening and sealing methods such as thread forms and face-sealing o-ring grooves respectively, which current AM technology is not capable of producing reliably. Therefore, a combination of AM and TM practices are used to manufacture the manifold. The major geometry of the manifold structure design itself along with all fluid tubing are built in the AM printing process. Extra material is printed on and around each component interface, creating an "as-printed structure". Figure 13 shows the as-printed structure with material test specimens after one of the completed prints. After printing and fluid passage clean-out, TM processes are used to shave away the extra material and manufacture the necessary interface features such as surface finishes, flatness, sealing grooves, and fastener thread forms.

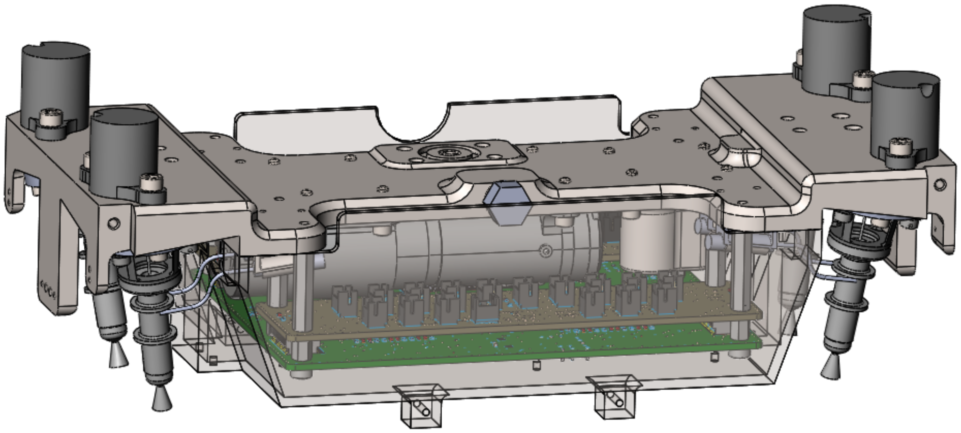

Fig. 12 Manifold interfacing components

Fig. 13 One of the four flight-grade manifolds after L-PBF printing, Credit: Volunteer Aerospace Inc.

C. Additional Hardware

While the propellant tank halves, PMDs, and manifold are the major components of the propulsion system that took a majority of the design consideration, a few additional custom-designed parts are essential to the system's functionality, the first of which is the recirculation block. As discussed in the Section III.B, a majority of the propellant flow travels through the recirculation loop during nominal conditioning and firing. For this recirculation loop to function as intended, a flow control device (fixed orifice in this case) is placed in the reciruclation loop, as seen in the propulsion schematic in Figure 7. Typical COTS orifices are designed to be installed into fluid tubing for proper functionality, however with the manifold having its fluid tubing 3D printed directly into its structure, there is no location to install an orifice. Instead, the recirculation block is designed as a separate part to house the orifice and make installation easy, while not creating any discontinuities in the fluid loop. Figure 14 shows how the recirculation loop is built to curve out of the manifold and into the recirculation block, through the orifice, and back into the manifold. Therefore, the orifice can be installed into the recirculation block as it is designed, and then the recirculation block can be installed onto the manifold to adapt to the system.

The next piece of additional hardware is known as the muffin tin. The muffin tin, in essence, is a protective cover to decrease the amount of space and thermal radiation soaked by the fragile electronic components during flight, such as the controller boards and pump. Radiation from the van Allen belts will be the largest dose of natural radiation the propulsion system wlll recieve, but another source will be from the thrusters themselves during firing. As the thrusters get up to +1600C during operation, they emit thermal radiation that could heat and damage the controller boards. A thermal analysis performed by MSFC showed that the muffin tin's angled walls near the thrusters absorb that energy and prevents from warming the boards. In addition, the bottom face of the muffin tin incorporates all of the spacecraft propulsion system +Z face interfaces, including mounting holes for the solar panels, low-gain antennas (LGAs), sun

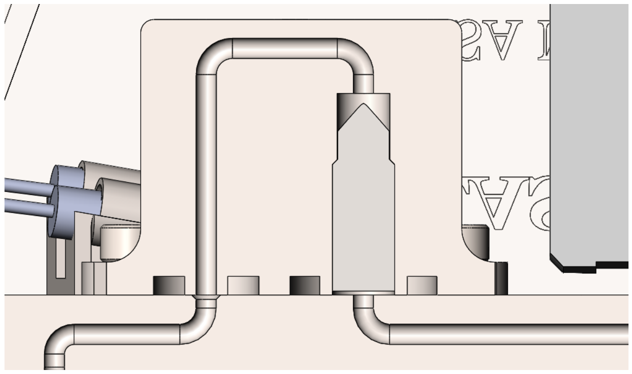

Fig. 14 Section view of the recirculation loop passing through the recirculation block

sensor, and deployment limit switch.

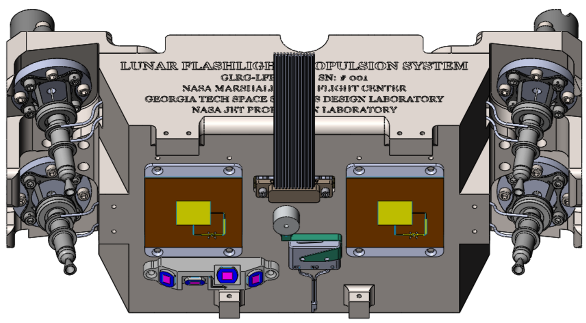

Fig. 15 Iso-view of the muffin tin showing all JPL hardware connections

Finally, each thruster junction box is held to the structure by a junction box mounting block and bracket. The mounting block has two symmetric cutouts angled in the direction of the thruster for ease of access and installation. As this block is in the highest heat zone of the system, it is made from titanium to prevent coefficient of thermal expansion (CTE) mismatch between a block of different material and the titanium manifold that could cause significant stress to the parts over many thermal cycles of thruster operation. Each junction box is wired to the thruster in a metal tube, which must be sized and bent precisely to match the location of the junction box mounting block. However, the small wires inside of the tubes places a bend radius restriction of 5mm on the heater cable and 3mm on the thermocouple cable. The junction boxes are epoxied to the cutouts on the mounting block, and finally each junction box bracket is fastened to the mounting block as a final precautionary measure to ensure the junction boxes do not come loose during launch if the epoxy broke.

V. Manufacturing Processes

A. Traditional Manufacturing

Design for traditional manufacturing (TM) was considered for all traditionally machined parts in the LFPS design - propellant tank halves, muffin tin, junction box blocks, PMD vanes. Traditional subtractive manufacturing techniques form parts by removing material from a material stock by means of various different types of machines such as mills, lathes, drill presses, water jets, and others. Computer Numerical Control (CNC) machines have been established on many of these machines as the main system by which large, complex parts are traditionally manufactured, with smaller touch-ups being fabricated by the hand-controlled machines. CNC machines are designed to be computer-controlled with 3-5 degrees of freedom in movement (axis control), which allow them to reliably achieve high-precision manufacturing dimensions in a fraction of the time of hand-controlled machines.

While these state-of-the-art TM machines are incredibly advanced, any subtractive manufacturing process has

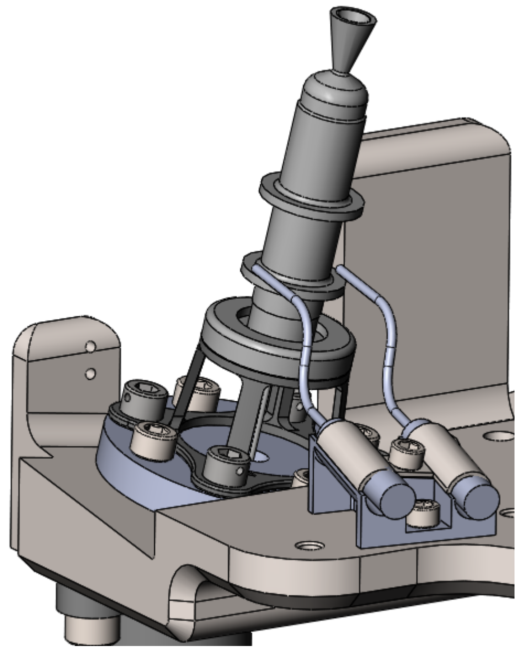

Fig. 16 CAD model of a thruster junction box (heater and thermocouple) being secured by a custom-designed titanium mounting block and bracket

limitations on what features are able to be produced and this fact must be considered during any part's design phase. Typical traditional manufacturing machines use high-speed drills of various shapes, sizes, and materials to remove material from the edge of a surface. This method requires that the tooling come in from one direction to shave away material, whether in a straight-line or while the part itself is spinning as on a lathe, essentially requiring a "line-of-sight" to cut away material from a surface. These methods are good for most features on most parts, but become extremely difficult, if not impossible, to create curving passages, overhangs, or other features that do not provide line-of-sight.

Because of this limitation, line-of-sight is one of the most important concepts in design for TM. The tank was decided to be TM via the NASA safety and fracture control boards (see Section IV.A), which required the tank be split into multiple parts as it is inherently a closed vessel. The tank is split into two parts, with the inner geometry of each tank half being produced by machining into the material stock in one direction with no designed overhangs. When the two parts are interfaced along their outer-edge, the machined geometries form the closed vessel for storing propellant. The process by which these two pieces are permanently joined together is discussed in Section V.C.

As an example of design for traditional manufacturing, TM was originally explored as an option for the LFPS recirculation block. The traditional manufacturing design is shown on the left, while the additively manufactured flight-level recirculation block is shown on the right. The TM recirculation block design required that each passage be drilled in a straight line, in this case also containing passages for the pump inlet and outlet. In contrast, the designed flight recirculation block is unable to be traditionally manufactured due to the curvature of the single passage from one side to the other, a geometry which a drill or any other TM technique would be unable to produce. However, the curved passage is preferred for this small-scale fluid application, with similar geometry seen in the internals of the manifold, both of which could not levy TM methods for manufacturing.

B. Additive Manufacturing

As opposed to traditional subtractive manufacturing, additive manufacturing builds parts by adding material where necessary. Lunar Flashlight utilized one of the most commonly used techniques for metal AM called laser-powder bed fusion (L-PBF), also called Direct Metal Laser Sintering (DMLS). This process works by using a high-power laser focused onto a bed of fine metal powder, which melts a small area of the powder. Before the powder can cool and solidify, the laser melts an adjacent area of powder and the melted powder cools together to form a solid piece of fused

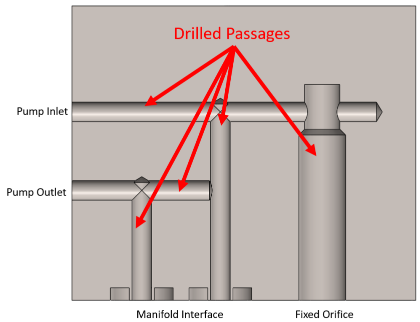

(a) TM Recirculation Block Idea

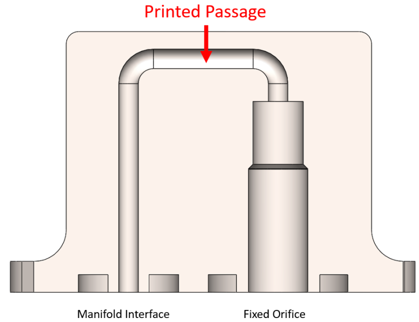

(b) Flight, AM Recirculation Block

Fig. 17 Two recirculation block designs with differing manufacturing techniques

metal. This occurs continuously throughout one layer of the print. After one layer is complete, the bed with the sintered layer moves slightly down and a new layer of metal powder is added on top to form the next layer of the print. This process repeats until the parts are formed.

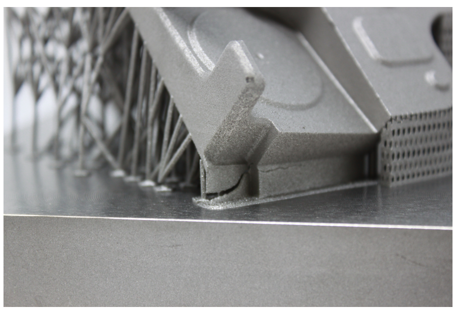

(a) Support material failure

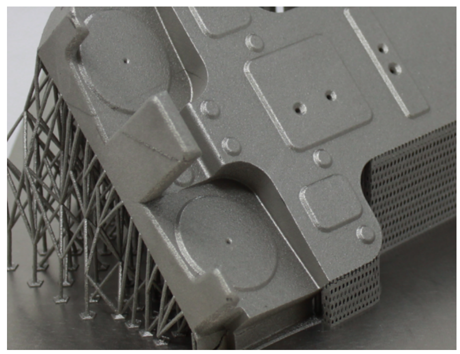

(b) Skipping line due to failure

Fig. 18 Failure seen in pathfinder manifold print

Similar to other 3D printing processes, L-PBF builds from the bottom-up. Therefore, support material is built into the print to support overhangs and other challenging features. For spaceflight applications, virgin metal powder is required which is very expensive. To minimize the use of powder and therefore cost, L-PBF flight parts are printed in an orientation that minimizes the amount of support material to be used while also providing the most stable base to minimize the risk of the part failing during printing due to loss of structural support or thermal distortion. The support material, seen on the left hand side of Figure 13 is built like scaffolding, all intertwined together and supporting the overhanging material.

One difficulty encountered during fabrication was a failure of the pathfinder manifold print due to the support material failing, as seen below in Figure 18a. The support material was broken was on the bottom of the manifold print which supported the left-hand side of the structure. A sharp corner was designed into the interface between this support material and the build plate, which failed during printing when the weight of the part created a stress concentration at the corner above the ultimate stress of the support material. Future builds ensured that each sharp corner was rounded to spread the load and provide necessary support structure. Figure 18b shows the how the failure affected the print. The part moved due to the failure and caused a discontinuity about halfway through the print, seen by the line that crosses the entire part along it's build plane.

A notable difference between plastic and metal 3D printing is the ability to machine the parts post-printing. Plastic parts are generally printed directly to their final versions. As an example, the BioSentinel propellant tank was printed to its flight version, and any necessary interfaces with sensors and electronics boards were machined from metals using traditional techniques. However, the manifold on the LFPS is the primary interfacing component of the assembly, so many precision threadforms and o-ring grooves need to be machined into the structure itself, as stated in Section IV.B.

Therefore, the structure that comes from the DMLS machine is called the "as-printed" structure, and is sent to a machine shop to become the flight-level, "as-machined" structure. During the print, additional material is designed into the as-printed structure on top of and around any machined interfaces. This includes threadforms, o-rings grooves, and important interfacing datums.

Traditional machining processes require that features be dimensioned from established datums, but if the major datums of a structure are covered in printed material that needs to be machined away, it is not obvious where the machining datum lies inside the part. To this end, the part is structured-light scanned to determine where the CAD model lies within the printed part. This helps the machine shop determine how much material is needed to machine to establish the major datums to then machine the rest of the part. A NASA-designed CubeSat green propulsion system was printed that was subject to structured-light scanning to show an example of the results of this process, as seen in Figure 19. In this case, the entire structure was printed with no necessary machining, so the heat map from the structured-light scanning shows the as-printed deviation from the CAD model.

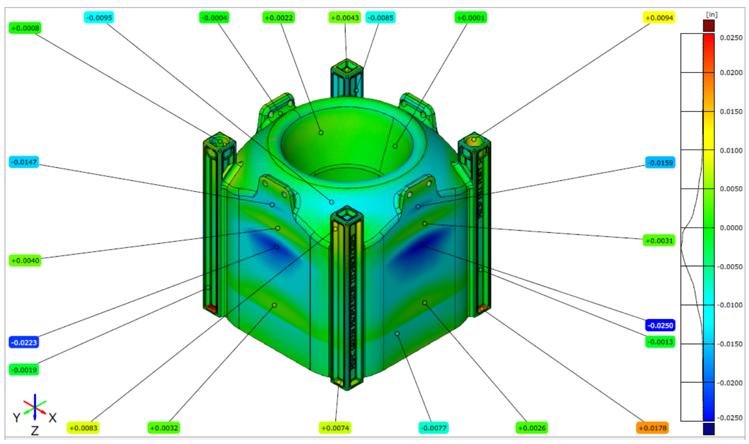

Fig. 19 MSFC-developed DMLS cubesat propulsion system, Credit: NASA MSFC

The Lunar Flashlight pathfinder and flight unit manifolds saw similar issues when structured-light scanned. Due to the orientation of the build, the middle of the manifolds near the pressure sensor tended to warp in the -Z direction, which also pull the X faces in the +Z direction as well as inwards, creating a concave curvature. For the SN 001 flight unit manifold, this deformation was unacceptable, but SN 002 and 003 are currently undergoing structured light scanning during the submission of this report to determine the magnitude of their warping. In the worst case scenario, all three flight manifolds may have to be reprinted, possibly in a new orientation or with more structural support material to diminish the amount of warping throughout the part. The pathfinder manifold was warped less than the flight manifold, so it will continue through the manufacturing process to prepare the manufacturing shop for the flight parts.

C. Electron-Beam (EB) Welding

The tank top and tank bottom structures are joined along a 360-degree weld-line seen in the middle of Figure 8, due to the TM-nature of the tank halves. There are many different types of welding used in industry, but electron beam welding was determined to be the best method for the LFPS. This conclusion was reached due to the factors of heat input during the welding process and the weld joint's size. Processes like friction stir welding and tig welding input massive amounts of heat during the welding process, which causes the metal to expand and then contract when cooled, which can affect material properties and overall dimensions that need to be exact for the small-size of the LFPS. Electron beam welding, by comparison, does not use nearly as much heat, which diminishes this concern. Additionally, electron beam welding is automated and intended for high-precision applications, while friction stir and tig welding are mainly utilized on much larger systems where the range of deformation is allowed to be much larger.

The weld geometry is a lap-joint design as seen in Figure 20. The lap-joint design allows for good weld penetration while also preventing FOD generated during the welding process from being blown into into the tank, which could clog up the fluid lines or cause damage to the system components. Because the lap-joint goes 360-degrees around the weld line, the fit-up is heavily dependent on the tank top and tank bottom tolerancing. As an example, there is a horizontal gap between the tank top and tank bottom weld steps that form the lap-joint. Nominally this gap is 0.003" wide with a

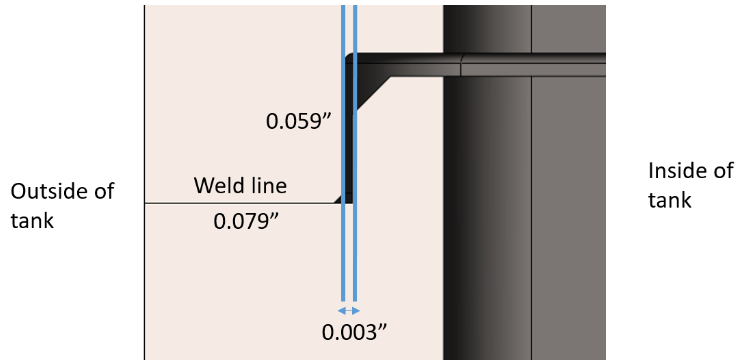

Fig. 20 EB weld lap-joint geometry

0.002" profile tolerance around the whole weld line. This prevents this gap from ever interfering as the minimum gap would be 0.001" and the maximum would be 0.005". This tolerance proved to be difficult to achieve, with a profile tolerance nonconformance seen on the pathfinder tank top and tank bottom structure causing the two pieces to not fit together as intended. Luckily, the manufacturing shop was able to fix this issue for the flight units. Additionally, the vertical tolerance was designed knowing that the EB weld vendor (EB Industries) was able to accept a weld-line gap of up to 0.003", but preferred no gap at all. To meet this feature, the tolerances were designed so that two structures could only possibly interfere by 0.001" if both parts were at worst case tolerance, which would create a 0.001" gap between the two structures along the weld-line.

The first issue encountered during EB welding of weld coupons was due to the chamfer seen on the back-weld step in Figure 20. Originally the chamfer was much smaller, and the tolerance band allowed the parts to interfere if the concave radius on the back step was large and the chamfer was small, creating a larger gap along the weld-line than designed for as previously discussed. Therefore, the next set of weld-coupons opened up that chamfer to prevent this issue from happening, and since this chamfer is not a part of the weld-line it did not affect weld penetration.

Another issue seen on the newer weld coupons after fixing the chamfer geometry was due to porosity and burn through of the weld through the wall, which required dialing in the weld parameters. EB welding requires that a beam of electrons be balanced in terms of energy, amplitude, frequency, and wave form. The weld samples were tested on to determine what combination of these parameters created the best weld for the project's geometry and application. The vendor initially found that when they got good penetration without burning through, they would find porosity rampant throughout the weld, but when they would try to get rid of the porosity they would burn through the wall.

The solution to this issue came from suggestions by weld engineers at MSFC. The initial samples delivered to the vendor were two inches long and were fixtured and insulated at either end when welded. The porosity was partially due to a lack of heat being applied, but if too much heat was applied then burn through would occur. Typical welds happen in single or multiple long passes, where the heat applied at one end is usually so far from the opposite end that the heat is unable to soak through the weld length and affect it. However, if the samples are short enough and insulated on both sides, as seen in the original weld samples, the heat could soak and cause higher heat loading throughout the part than expected, leading to burn through. With longer passes (a longer sample, more like the LFPS propellant tank weld-line itself) enough heat can be applied to prevent porosity but very little heat will soak from one end of the line to the other, preventing burn through. The failed samples are shown in Figure 21 and the passed samples with the finalized weld parameters are shown in Figure 22.

D. Cleanliness Standards

An item not discussed until the manufacturing phase of the project was the concept of establishing and maintaining cleanliness from the end of manufacturing through integration and testing. Typically the GT SSDL has operated on a best-effort cleanliness basis using a combination of cleanroom environments and thorough cleaning with isopropyl alcohol. NASA wanted to have a quantifiable level of cleanliness, which must be established and inspected to conform to a cleanliness standard. The project baselined the IEST-STD-CC1246E specification for precision cleaning, meeting Level 100 and no particles greater than 50 microns for all wetted components including the propellant tanks, manifold, recirculation block, valves, and pump. Non-wetted hardware was not required to meet the same cleanliness level, and instead is cleaned based on GLRG-SOP-01-Flight Hardware Cleanliness procedure.

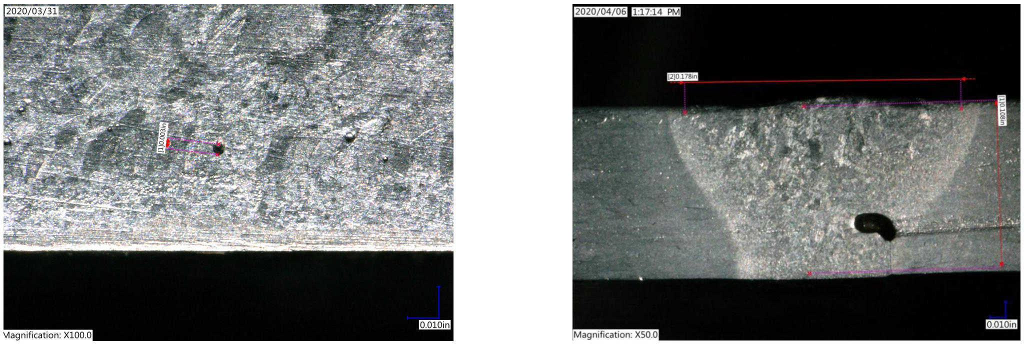

(a) Porosity example **(b) Burn through example**

Fig. 21 Failed weld coupons during weld parameter development

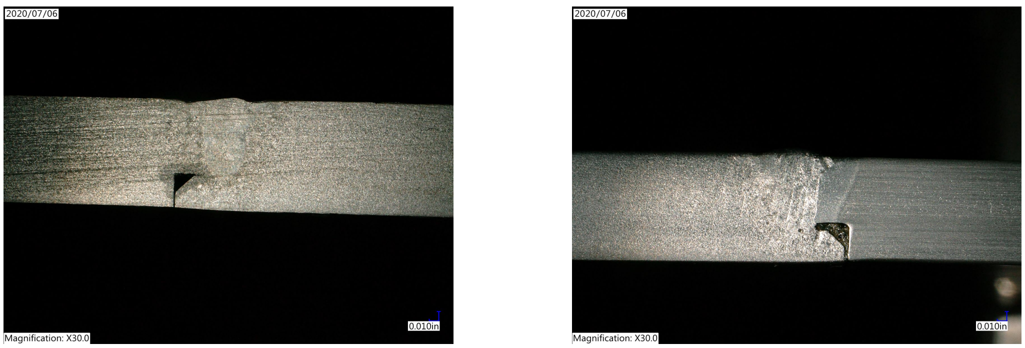

(a) Sample 1 **(b) Sample 2**

Fig. 22 Final weld samples with flight parameters. Varying color between the two samples is due to one sample being cut in the direction of the stock grain, the other being cut perpendicular to the grain direction

The wetted geometry that required meeting the cleanliness specification required communication with vendors and cleanshops to ensure the precision cleaning was conducted prior to integration steps being conducted. The propellant tanks were precision cleaned prior to delivery to GT by requesting that Xometry (the manufacturing shop) find a precision clean shop to do the process before shipment. The same occured with the manifold, printed by Volunteer Aerospace, machined by MicroCraft, and cleaned by Technical Micronics Control, Inc. (TMC). The recirculation blocks were cleaned after machining, but will be recleaned after fixed orifice installation at Lee Company and proof testing at MSFC. The tanks do not need to be recleaned after proof testing as the internals are sealed during the pressure testing by using cleaned GSE hardware (blanking plates).

VI. Integration and Test

A. Procedure Development

The LFPS integration and test procedures were developed by the Georgia Tech SSDL with input from NASA MSFC. Part of the reason the GT SSDL was placed on the LFPS project was due to GLRG's prior experience on the BioSentinel mission, which required the development of detailed integration procedures. The procedures focus on outlining all necessary integration steps, quality assurance (QA) witness steps, torque value recordings for each fastener on the system, and a multitude of pictures to document the integration process. The procedures also list all necessary parts, equipment, and documentation needed, as well as specifying the qualities of a safe, clean environment necessary for integration.

The LFPS integration procedures were developed following these guidelines, and are are called Assembly, Integration and Test Procedures (AITPs). The LFPS integration requires nine of these, which are outlined in Table 3.

Table 3 LFPS Assembly, Integration and Test Procedures

Procedure	Description
AITP-01	PMD sponge, vane, filter installation into tank bottom
AITP-02	Propellant tank EB-welding, proof and burst testing
AITP-03	Recirculation block orifice installation, proof and burst testing, precision cleaning
AITP-04	Recirculation block, thruster valves, pressure sensor. heater, TC installation into manifold, leak test
AITP-05	Fill/drain valve, pressure sensor, bulk prop iso-valve, heater, TC installation into welded tank, leak test
AITP-06	Tank and manifold subassembly joining, leak test
AITP-07	Pump installation, leak test
AITP-08	Controller installation
AITP-09	Thruster installation, system level leak test

B. Proof and Burst Testing

Pressure testing is a way of testing the strength of the system and validating the structural analysis, which is important for qualifying the propulsion system for flight. The LFPS project conducts pressure testing at the component-level before integration with any other flight hardware, essentially testing each part of the system to ensure that it will not damage other components when under pressure.

There are two main types of pressure testing for the LFPS components: proof and burst testing. A proof test exposes the internals of the hardware to proof pressure as defined in the Level 4 Requirements seen in Table 2. To pass a proof test, the component is allowed to deform elastically but not plastically. Burst testing subjects the component to 2.5xMDP and in this case the system is allowed to plastically deform but it is not allowed to fracture. If the component passes this pressure without failure, the burst test will proceed by ramping up the pressure past 2.5xMDP until the part does fracture. This tells the engineers where the failure point is on that component, and gives a finalized design margin.

Pressure and burst testing has not been conducted on this scale before on previous GLRG propulsion projects, mainly because the pressures were quite low and the systems were made from 3D printed plastic rather than metal. Currently, the SSDL does not have the capability to conduct this pressure testing safely. Therefore, these tests are being performed on the LFPS at NASA MSFC, but more pressure testing campaigns could be conducted at Georgia Tech depending on future facility abilities and personnel.

C. Leak Testing

Another major test to be conducted during the test plan are the regular leak tests at the end of each integration step involving newly-integrated components featuring fluid seals. Leak tests measure the rate of gaseous leakage of a fluid seal, and this rate is defined in the system-level requirements. If too much gas is allowed to leak, the system will depressurize over time and will either have reduced performance or stop working all together.

Leak testing requires that the system be raised to the maximum expected operating pressure (MEOP) or higher. The LFPS project requires leak tests be performed at 1.1xMDP (110 psia) while MEOP is around 70 psia. A higher gas pressure will force more gas out of any small openings which increases the measured leak rate. If the system meets the leak requirement at an elevated pressure, it will also meet it at a lower pressure so this is a conservative method to ensure the system meets the requirement.

Measuring the leak rates and locating the leaking seals around the system is challenging. Quantifying leak rates typically requires the use of a "sniffer" or mass spectrometer, which take measurements of the chemicals it senses over time and uses that data to find an average leak rate of the system. The sniffer can be used in the atmosphere but the mass spectrometer typically is used when hooked up to a vacuum chamber to get the best measurement of total leak rate.

Because of the complex steps involved with setting up the mass spectrometer to the vacuum chamber, many of the earlier leak tests will be conducted qualitatively using a bubble test. The bubble test involves placing a bubbling liquid mixture around the externals of a fluid seal while the internals are pressurized, and any escaping gas will be caught in the mixture and create visual bubbles. Any visual bubbles seen will show a leak that is much too large to meet the

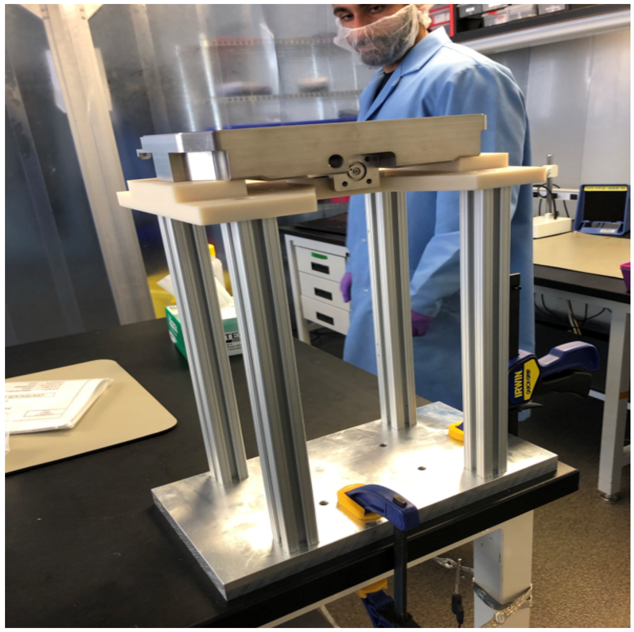

Fig. 23 AITP-01 MGSE stand showing the machined common stand and the AITP-specific 3D printed fixture interfacing to the pathfinder tank bottom

requirement, and the seal will have to be fixed.

D. Mechanical Ground Support Equipment (MGSE)

On larger projects, mechanical ground support equipment requires significant design effort over a large period of time to ensure that the heavy, large spacecraft will be adequately supported during the integration and transportation processes. Due to the small size and low mass of CubeSats, the MGSE development is typically much easier. However, it needs to be considered for important integration steps to ensure that the assemblers have a clean and useful support structure to assist in the integration process.

Past projects in the GT-SSDL have utilized different custom MGSE designs specific to their missions. These MGSE structures have ranged from stands made completely of t-slotted framing to stands made of plastics. However, many of the past projects have not required multiple assemblies to happen simultaneously in many different configurations and orientations, which is what is required for the integration of the LFPS. Because of this, many different stands specific to each integration step needed to be designed and built.

The LFPS MGSE is designed to reduce the number of individual stands needed to be built while also providing the flexibility to easily transition between one integration stand to another. This result was accomplished by using a combination of traditional and additive manufacturing. A common structure to each MGSE stand was made from a machined aluminum plate and four one-foot tall t-slotted frames tapped on either end with 1/4-20 threads. The bottom of the aluminum plate has counterbore for 1/4-20 socket head cap screws to sit in and also have the bottom face be flush with any surface it is placed on. The screws stick through the top face of the plate and interface to the t-slotted frames. Next, a 3D-printed structure is designed to interface with the hardware for a specific integration step, which has a four bolt counterbore design to interface with the top face of the four t-slotted frames. In this way, only one common stand is needed for all integration, and it is quite easy to remove the 3D-printed fixture and replace it with another integration step's fixture. A picture of the MGSE stand with the AITP-01 fixture is shown in Figure 23.

Two common stands were built to allow for two assemblies to occur simultaneously during integration, as there are a minimum of two people required to conduct the integration steps. Three more 3D-printed fixtures are being designed and prototyped for the remaining AITPs. One will be needed for AITP-04, one for AITP-05, and a final one for AITP-06 through AITP-09. AITP-06 joins the tank subassembly and manifold subassembly, and then all remaining steps build onto the manifold but do not touch the tank. Therefore, the assembly can remain in the same orientation for the remainder of the integration process.

VII. Future Design Considerations

There were many lessons learned throughout the development phase of this project, some good and some bad. These lessons can be applied to future projects within GLRG to make the designs better and help streamline the project development.

One of the major improvements that could be made is to incorporate more elements of the design into a single continuous AM structure, depending on future development of AM processes. This would help remove significant design complexity and many necessary processes due to the mixed nature of TM and AM being used around the system such as EB-welding. However, the materials science of AM still has a bit of growing room as seen with the manifold structured-light scanning issues. However, having the capability to combine the tank and manifold would rapidly speed up the CubeSat propulsion system development process.

Next, with more AM flight heritage and increased understanding of how strong and reliable AM metals are, more AM parts such as the manifold can be heavily mass optimized to only have material added where necessary for structural and functional reasons. This was explored for a time on LFPS, but was too late to implement while also trying to meet the project's tight manufacturing delivery and integration schedule. However, future iterations of the LFPS or systems like it should consider mass-optimization early in the design phase. MSFC regularly uses mass-optimization codes to determine where material can be removed without harming the part or decreasing its strength margins below acceptable levels. This approach may also be another interesting area for future research projects that could be utilized on many structures, especially in the space industry where mass is such an important aspect of design.

Next, the issue of securing the thruster junction boxes caused the rapid development of a new part at the same time as manufacturing of the manifold was beginning, which was not ideal. This issue was not caught until late in the project due to miscommunication. However, a big lesson learned during this issue was how the junction boxes can be routed. Because the junction boxes have minimum bend radii and have a specified length, the structural designer, system integrator, and thruster developer must communicate about how the thrusters fit in the system and where the junction boxes could feasibly sit. An avenue that could be explored in the future is to remove material in one of the structures to seat the junction boxes in with epoxy, and then have a bracket fastened to the structure by a single bolt in the middle of the junction box mounting cutouts. This was explored on the LFPS, but due to the manifolds already being printed by the time this issue was resolved, the decision was made to create a separate part rather than make many major cutouts in the geometry post-printing.

VIII. Lunar Flashlight's Path Forward

At the time of this report, three flight propellant tank top and bottom structures have been delivered from Xometry to Georgia Tech, and AITP-01 is underway. Immediately following AITP-01, the tank halves including the PMD will be shipped to EB Industries for electron beam welding, after the weld process is qualified and the pathfinder tank has been welded. The as-machined flight recirculation blocks have been delivered to GT and have been shipped to the Lee Company for orifice installation, to be followed by proof, burst testing and precision cleaning.

The remainder of the project will consist of finishing the manufacturing process on the manifolds and ordering other hardware needed later in the assembly, particularly the muffin tin and junction box mounting blocks and brackets. Proof and burst pressure testing will be conducted in Fall 2020 at MSFC on the welded tank assemblies, manifolds, and recirculation blocks. As these processes finish, the hardware will be returned to GT and the GLRG propulsion team will conduct AITP-04 through AITP-09 along with all necessary tests. If possible, engineers and designers from Plasma Processes Inc., Flight Works Inc., and MSFC will come to GT to install their custom-designed parts for the system (pump, thrusters, valves). After all integration steps and tests have been conducted, the completed assembly will be shipped to JPL in Pasadena, California where it will be integrated with the Lunar Flashlight spacecraft. All functional and environmental tests will be conducted within the full spacecraft assembly at JPL to prepare for flight, which is currently scheduled for mid-2021 but could see delays due to the global pandemic. After delivery to JPL, the GT-SSDL will remain on the LFPS project for support as necessary, but all hardware will be out of lab.

IX. Conclusions

With assistance and support from NASA's Marshall Space Flight Center and the Jet Propulsion Laboratory, an AF-M315E green monopropellant propulsion system was developed by the Georgia Tech Space System Design Laboratory for NASA's Lunar Flashlight CubeSat mission. A pump-fed fluid schematic is utilized so that necessary system pressures are low, reducing the risk of the propulsion system to the launch vehicle and the necessary steps to pass safety and fracture control reviews. A combination of traditional and L-PBF additive manufacturing creates the components of the LFPS, with the AM manifold housing most of the fluid passages that are printed directly into the structure, adding to the space-flight heritage of AM. Challenges during the design, fabrication and assembly phase led to many learning opportunities, including overcoming difficulties seen with TM, AM, EB welding, and many more that were mostly specific to scaling a green monopropellant propulsion down to the size of a CubeSat. Upon submission of this report, the project is starting to transition from the manufacturing phase into the integration phase, with expected delivery to JPL in early 2021, barring any delays. If all goes according to plan, the custom-designed Lunar Flashlight Propulsion System will place the Lunar Flashlight spacecraft into polar Lunar orbit by the end of 2021, and allow for a 90-day science mission with possibility for a mission extension.

X. Acknowledgements

I have to thank the plethora of people around me that have made reaching this point in my life and career a reality. First, my parents Lisa and Michael Huggins who raised me to reach for the stars and providing me the emotional (and financial!) support to really go for it. Next, all of my friends from different walks of life that support me every day. Dawn Andrews, for being the best mentor I could ask for and a fantastic friend along the way (see you in LA!); Ali Talaksi, for listening to my ramblings and providing the most relevant Stephen A. Smith memes I could have never imagined enjoying more; Nathan^2 and Sterling Peet for tackling the other end of this amazing project with a completely different set of knowledge and incredible dedication; the undergrad troopers - Mackenzie Glaser, Sahaj Patel, Lacey Littleton, Logan Skimore - for doing more than I ever did in undergrad.

A huge thanks go to the entire NASA MSFC family - Daniel Cavender, Don McQueen, Hunter Williams, Carlos Diaz, and others - for building my knowledge base, providing me with more responsibility than I knew what to do with, and helping me grow to bigger and better heights. And last but not least, to Dr. Glenn Lightsey for harboring the most exciting, fun, and dedicated lab at Georgia Tech, the graduate school opportunity of a lifetime, and the advisement along the way.

A thanks go out to all of the subvendors who made this project a reality and a pleasure to work on: Xometry, Volunteer Aerospace Inc., EB Industries LLC, Plasma Processes Inc., Flight Works Inc., The Lee Company, and the multitude of others involved that are not mentioned here.

I finally would like to acknowledge the Jet Propulsion Lab Subcontracts No. 1631930, 1651241 and NASA Cooperative Agreement 80MSFC19M0044 that have funded the work on the Lunar Flashlight Propulsion System at the Georgia Tech SSDL.

References

[1] Wilk, M. D., and Lightsey, E. G., “Development of Maneuverable Deep Space Small Satellites Development of Maneuverable Deep Space Small Satellites,” Tech. rep., May 2019.

[2] Andrews, D., and Lightsey, E. G., “Design of a Green Monopropellant Propulsion System for the Lunar Flashlight Mission,” Tech. rep., Dec. 2019.

[3] Cohen, B. A., Hayne, P. O., Greenhagen, B., Paige, D. A., Seybold, C., and Baker, J., “Lunar Flashlight: Illuminating the Lunar South Pole,” *IEEE Aerospace and Electronic Systems Magazine*, Vol. 35, No. 3, Mar. 2020, pp. 46–52.

[4] Andrews, D., Huggins, G., Lightsey, E. G., Cheek, N., Lee, N. D., Talaksi, A., Peet, S., Littleton, L., Patel, S., Skidmore, L., Glaser, M., Cavender, D., Williams, H., McQueen, D., Baker, J., and Kowalkowski, M., “Design of a Green Monopropellant Propulsion System for the Lunar Flashlight CubeSat Mission,” *34th Annual Small Satellite Conference*, Aug. 2020.

[5] Spores, R. A., Masse, R., Kimbrel, S., and Mclean, C., “GPIM AF-M315E Propulsion System,” *50th AIAA/ASME/SAE/ASEE Joint Propulsion Conference & Exhibit*, Cleveland, Ohio, Jul. 2020, pp. 1–12.

[6] Sampson, J. W., Martinez, J., and Mclean, C., “Fracture Mechanics Testing of Titanium 6Al-4V in AF-M315E,” *51st AIAA/SAE/ASEE Joint Propulsion Conference*, Orlando, FL, Jul. 2015, pp. 1–14. doi:10.2514/6.2015-3756.

[7] Hartwig, J. W. N. J. H. G. R. C., “Propellant Management Devices for Low-Gravity Fluid Management: Past, Present, and Future Applications,” *Journal of Spacecraft and Rockets*, Vol. 54, No. 4, Apr. 2017, pp. 808–823. doi:10.2514/1.A33750.

[8] Lightsey, E. G., Stevenson, T., and Sorgenfrei, M., “Development and Testing of a 3-D-Printed Cold Gas Thruster for an Interplanetary CubeSat,” *Proceedings of the IEEE*, Vol. 106, No. 3, Feb. 2018, pp. 379–390. doi:10.1109/JPROC.2018.2799898.